PCCP

Cite this: *Phys. Chem. Chem. Phys.*, 2011, **13**, 2409–2416

www.rsc.org/pccp

PAPER

Ionization-induced π → H site switching dynamics in phenol–Ar_3

Shun-ichi Ishiuchi,[a] Mitsuhiko Miyazaki,[a] Makoto Sakai,[a] Masaaki Fujii,*[a] Matthias Schmies[b] and Otto Dopfer*[b]

Received 24th September 2010, Accepted 9th November 2010
DOI: 10.1039/c0cp01926g

Electronic excitation spectra of the $S_1 \leftarrow S_0$ transition obtained by resonance-enhanced two-photon ionization (REMPI) are analysed for phenol–Ar_n (PhOH–Ar_n) clusters with $n \leq 4$. An additivity rule has been established for the S_1 origin shifts upon sequential complexation at various π binding sites, which has allowed for the identification of two less stable isomers not recognized previously, namely the (2/0) isomer for $n = 2$ and the (2/1) isomer for $n = 3$. Infrared (IR) spectra of neutral PhOH–Ar_n and cationic $PhOH^+$–Ar_n clusters are recorded in the vicinity of the OH and CH stretch fundamentals (ν_{OH}, ν_{CH}) in their S_0 and D_0 ground electronic states using IR ion dip spectroscopy. The small monotonic spectral redshifts $\Delta\nu_{OH}$ of about -1 cm^{-1} per Ar atom observed for neutral PhOH–Ar_n are consistent with π-bonded ligands. In contrast, the IR spectra of the $PhOH^+$–Ar_n cations generated by resonant photoionization of the neutral precursor display the signature of H-bonded isomers, suggesting that ionization triggers an isomerization reaction, in which one of the π-bonded Ar ligands moves to the more attractive OH site. The dynamics of this isomerization reaction is probed for $PhOH^+$–Ar_3 by picosecond time-resolved IR spectroscopy. Ionization of the (3/0) isomer of $PhOH^+$–Ar_3(3π) with three π-bonded Ar ligands on the same side of the aromatic ring induces a π → H switching reaction toward the $PhOH^+$–Ar_3(H/2π) isomer with a time constant faster than 3 ps. Fast intracluster vibrational energy redistribution prevents any H → π back reaction.

1. Introduction

Clusters of phenol (PhOH) are ideal model systems to investigate the subtle competition between different binding motifs of aromatic molecules, as the ligands can bind either to the OH group *via* hydrogen bonding (H-bond) or to the π-electron system of the aromatic ring (π-bond).[1–10] H-bonding to PhOH is mainly stabilized by electrostatic and inductive forces, whereas dispersion interactions provide the major contribution to the attractive part of the potential for π-bonding. The preference for H- or π-bonding sensitively depends on the polarity of the ligand, the degree of microsolvation, the substitution of functional groups, and the charge or protonation state of PhOH. In general, neutral acidic aromatic molecules interact with nonpolar ligands preferentially *via* π-bonding, as dispersion dominates the attraction. However, ionization or protonation leads to preferential H-bonding to the acidic functional group due to additional electrostatic and induction forces arising from the excess charge. This charge-induced π → H switch is a general phenomenon for acidic aromatic molecules interacting with nonpolar ligands,[8] and has been established for a variety of aromatic molecules featuring acidic NH and OH proton donor groups.[11–18]

The present work investigates the structures of the PhOH–Ar_3 complex in the neutral (S_0) and cation (D_0) ground electronic states and the dynamics of the π → H switch induced by the ionization process using IR spectroscopy. For this purpose, we briefly summarize the current knowledge of phenol–Ar_n clusters, which have been investigated up to $n = 3$. A variety of spectroscopic[2,6,19–21] and quantum chemical studies[22–24] demonstrate that PhOH–Ar has a π-bonded global minimum structure in the S_0 state, denoted PhOH–Ar(π). The experimental dissociation energy of $D_0(\pi) = 364 \pm 13$ cm^{-1} [25] is in good agreement with values from state-of-the-art quantum chemical calculations at the CCSD(T)/CBS level, $D_0(\pi) = 389$ cm^{-1}.[23] The H-bonded dimer, denoted PhOH–Ar(H), is predicted to be a less stable transition state connecting the two equivalent PhOH–Ar(π) minima *via* a barrier of ~250 cm^{-1},[23] and has not yet been identified experimentally. Similar to PhOH–Ar, for the PhOH–Ar_2 trimer only a single isomer has been identified so far in the molecular beam expansion,[20] and spectroscopy at the level of rotational resolution reveals a (1/1) structure with the two equivalent π-bonded Ar atoms attached to opposite sides of the aromatic ring, PhOH–Ar(2π).[21] Despite several studies in different groups,[20,21,26–28] no evidence has been presented so far for the presence of the less stable (2/0) isomer of PhOH–Ar(2π) in

[a] *Chemical Resources Laboratory, Tokyo Institute of Technology, Yokohama 226-8503, Japan. E-mail: mfujii@res.titech.ac.jp*
[b] *Institut für Optik und Atomare Physik, Technische Universität Berlin, Hardenbergstrasse 36, 10623 Berlin, Germany. E-mail: dopfer@physik.tu-berlin.de*

the supersonic expansion, in which both Ar atoms are located on the same side of the aromatic PhOH ring. At first glance, this is a surprising result, as the (2/0) isomer could readily be formed and identified for the related benzene–Ar_2 and aniline–Ar_2 complexes formed in similar molecular beam experiments.[29–31] For the PhOH–Ar_3 cluster, only vibrationally-resolved spectra are available and its configuration is less certain.[20,26,32] Photoionization and photofragmentation studies of PhOH–Ar_3 clearly demonstrate that all Ar ligands are π-bonded in the single isomer identified so far, PhOH–Ar_3(3π).[20,32] Although the observed isomer was initially assigned to the (2/1) isomer,[26] the size-dependent complexation shifts of the S_1 origin transitions suggest an assignment to the (3/0) isomer with all three Ar ligands on the same side of the aromatic ring.[32] The present work reports electronic excitation spectra of the $S_1 \leftarrow S_0$ transition of PhOH–Ar_n clusters with $n \leq 4$ obtained by resonance-enhanced two-photon ionization (REMPI). The S_1 origin shifts observed upon sequential complexation at various π binding sites are analysed using a model based on additivity rules. The development of this simple model has allowed for the identification of two less stable isomers not recognized previously, namely the (2/0) isomer for $n = 2$ and the (2/1) isomer for $n = 3$. Moreover, it supports the assignment of the (3/1) isomer observed in the REMPI spectrum of PhOH–Ar_n, which is reported here for the first time.

Spectroscopic[11,33,34] and theoretical studies[23,24,33,35] show that in the cationic D_0 state the H-bonded $PhOH^+$–Ar(H) dimer is the global minimum on the potential and more stable than the π-bonded $PhOH^+$–Ar(π) local minimum. The experimental binding energies of $D_0(\pi) = 535 \pm 3$ cm^{-1} [25] and $D_0(H) \approx 800$–900 cm^{-1} [11,27,32] are in accord with the interaction energies of 595 and 946 cm^{-1} obtained at the CCSD(T)/CBS level, respectively.[23] Thus, ionization of PhOH–Ar switches the energetic order of the π and OH binding sites. Therefore, spectroscopic techniques based on photoionization of neutral PhOH–Ar(π) prepare only the $PhOH^+$–Ar(π) local minimum due to vertical Franck–Condon factors and unravel mainly the spectroscopic properties of this less stable isomer.[2,25,26,32] This is in contrast to studies using electron ionization for generation of $PhOH^+$–Ar_n clusters, which predominantly produce the most stable cluster cation isomers leading to a solvation sequence, in which the initially formed $PhOH^+$–Ar(H) dimer is further solvated by π-bound ligands, $PhOH^+$–Ar_n(H/[n−1]π).[8,11,33] The ionization-induced π → H switch in the preferred binding motif in $PhOH^+$–Ar_n clusters leads to interesting photoionization and photofragmentation energetics, which have been investigated in detail for $n = 2$ and 3.[27,32,37–39] The involved isomerization processes have recently been characterized in real time by picosecond time-resolved spectroscopy for $PhOH^+$–Ar_2[38,39] and $PhOH^+$–Kr,[40] demonstrating that the dynamical behaviour strongly depends on the mass and number of the rare gas atoms, with respect to both the isomerization mechanism and the corresponding rate constants. The present work extends these studies to the larger $PhOH^+$–Ar_3 cluster.

2. Experimental techniques

PhOH–Ar_n clusters are generated in a molecular beam and investigated with a variety of spectroscopic techniques using nanosecond and picosecond laser systems, featuring pulse lengths of 5 ns and 3 ps, respectively. Details of the experimental setup, cluster generation, the spectroscopic methods, and the employed laser systems are given elsewhere.[39] Briefly, PhOH–Ar_n clusters are produced in a supersonic expansion of PhOH (40 °C) seeded in 5 bar Ar and ionized in the extraction region of a time-of-flight mass spectrometer *via* resonant two-color two-photon ionization (1 + 1′ REMPI). The first UV photon (ν_{UV}) excites clusters into the S_1 electronic state, whereas a second photon (ν_{ION}) is used for soft ionization with low excess energy to avoid fragmentation of the cluster cations. REMPI spectra are obtained by scanning ν_{UV} through the vibronic resonances of the S_1 state. Photoionization efficiency (PIE) spectra are obtained by fixing ν_{UV} to a particular S_1 resonance and scanning ν_{ION} through the ionization threshold of the cation ground state. The constant extraction field of 1 kV cm^{-1} implies a shift of −190 cm^{-1} for all ionization and fragmentation threshold energies due to pulsed field ionization of high-n Rydberg states. IR dip spectroscopy is employed to measure IR spectra of isomer-selected PhOH–Ar_n clusters in the S_0 or D_0 state by firing the IR laser prior or after the ionization lasers, respectively.

3. Results and discussion

3.1 REMPI spectra and S_1 origin shifts

The 1 + 1′ REMPI spectra of PhOH–Ar_n with $n \leq 4$ shown in Fig. 1 are in good agreement with previous studies for $n \leq 3$.[2,21,26,32] They were recorded employing a fixed frequency of $\nu_{ION} = 32\,260$ cm^{-1} to ensure soft ionization and avoid fragmentation. The S_1 origins of the predominant isomers at 36 350, 36 316, 36 281, 36 373, and 36 338 cm^{-1}

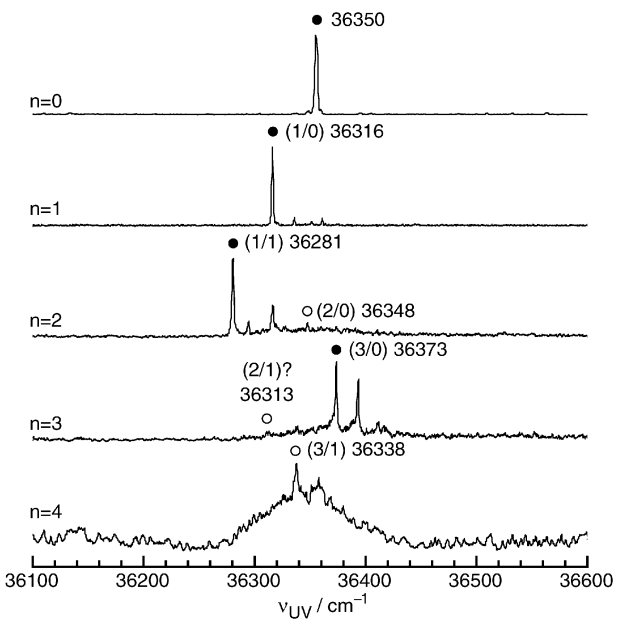

Fig. 1 1 + 1′ REMPI spectra of PhOH–Ar_n (n = 0–4) in the vicinity of the $S_1 \leftarrow S_0$ transition employing a fixed frequency of $\nu_{ION} = 32\,260$ cm^{-1} to ensure soft ionization. The (n/m) isomer assignments as well as the frequencies of the corresponding S_1 origins (in cm^{-1}) are indicated (Table 1). Filled and open circles indicate previous and new assignments, respectively.

imply absolute shifts of $\Delta S_1 = -34, -69, +23$, and -12 cm^{-1} for $n = 1$–4, respectively. The nearly additive redshifts for $n \leq 2$ are indicative of the (1/0) and (1/1) structures of PhOH–Ar(π) and PhOH–Ar$_2$(2π), whereas the absolute blueshift of the intense origin for $n = 3$ is indicative of the (3/0) isomer of PhOH–Ar$_3$(3π).[30–32] The weak origin at 36 313 cm^{-1}, corresponding to a total redshift of -37 cm^{-1}, is tentatively assigned in the present work to the hitherto unidentified (2/1) isomer of PhOH–Ar$_3$(3π), by analogy with the isoelectronic aniline–Ar$_n$ cluster series.[30,31] The hole-burning spectrum of PhOH–Ar$_3$(3π) is consistent with this view.[20] Following the assignment given above, the addition of the first, second, and third Ar ligand on a single side of PhOH induces incremental shifts of $\Delta S_1 = -34, +32$, and $+25$ cm^{-1}, respectively. Assuming additivity rules, this simple scheme predicts the S_1 origin of the hitherto unidentified (2/0) isomer at $\sim$36 348 cm^{-1} with essentially no total shift ($\Delta S_1 \approx -2$ cm^{-1}), and indeed there is a relatively intense band in the corresponding REMPI spectrum of PhOH–Ar$_2$. This transition has previously been assigned to an intermolecular combination band of the (1/1) isomer with a frequency of 67 cm^{-1}, and this isomer assignment was confirmed by hole-burning spectroscopy.[20] Nonetheless, it is conceivable that a further contribution to this band arises from the overlapping S_1 origin of the (2/0) isomer. Indeed, the relative intensity of this transition at 36 348 cm^{-1} seems to vary substantially in the REMPI spectra recorded in different studies,[20,21,26–28] providing further confidence that part of this band is due to the (2/0) isomer, whose relative population is expected to strongly depend on the various expansion conditions. As was shown in detail previously for aniline–Ar$_n$, the formation of different isomers strongly depends on the expansion conditions.[30] In particular, the Ar concentration is a sensitive parameter to control the ratio of isomers with solvation on a single side or on both sides, which also sensitively depends on the cluster size. The application of the above-mentioned additivity rules to the $n = 4$ cluster predicts absolute shifts of ~ -11 and -4 cm^{-1} for the (3/1) and (2/2) isomers, leading to expected S_1 origin bands at 36 339 and 36 346 cm^{-1}. Accordingly, the intense S_1 origin observed for PhOH–Ar$_4$(4π) at 36 338 cm^{-1} is attributed to the (3/1) isomer. As additional Ar atoms attached on the same side of PhOH induce incremental blueshifts for $n > 1$, the S_1 origin of the (4/0) isomer is expected to occur at frequencies larger than 36 375 cm^{-1}.[29] The broad background observed in the PhOH–Ar$_4$ spectrum is currently attributed to fragmentation of larger clusters after ionization.[26] Table 1 and Fig. 2 summarize the observed S_1 origin energies and compare the experimental ΔS_1 shifts with those extracted from the additivity model. As can be seen, the three input parameters of the model can reproduce all six observed transition energies to within 1 cm^{-1}, strongly supporting the isomer assignments. Interestingly, the S_1 transition frequency of PhOH isolated in a cryogenic Ar matrix (36 365 $\pm$ 15 cm^{-1})[41] is close to the gas phase value (36 350 cm^{-1}), implying only a small shift of $\Delta S_1 = 15 \pm 15$ cm^{-1} induced by complete solvation of PhOH in an Ar environment. Below, we concentrate on the PhOH–Ar$_3$(3π) isomer with the intense S_1 origin at 36 373 cm^{-1}, which is almost certainly due to the (3/0) isomer, probably consisting of an Ar$_3$ triangle stacked to the aromatic phenol ring.

Table 1 S_1 excitation energies and ΔS_1 shifts (in cm^{-1}) induced by Ar complexation for the various isomers of PhOH–Ar$_n$ for $n \leq 4$ are compared to the shifts predicted by the additivity model[a]

n	S_1 (exp)	ΔS_1 (exp)	ΔS_1 (model)	Isomer
0	36 350	0		
1	36 316	−34	−34	(1/0)
2	36 281	−69	−68	(1/1)
2	36 348	−2	−2	(2/0)
3	36 313	−37	−36	(2/1)
3	36 373	+23	+23	(3/0)
4	36 338	−12	−11	(3/1)
4			−4	(2/2)
4			?	(4/0)

[a] The model assumes incremental additive shifts of $\Delta S_1 = -34, +32$, and $+25$ cm^{-1} for the first, second, and third Ar ligand attached to a single side of PhOH, respectively.

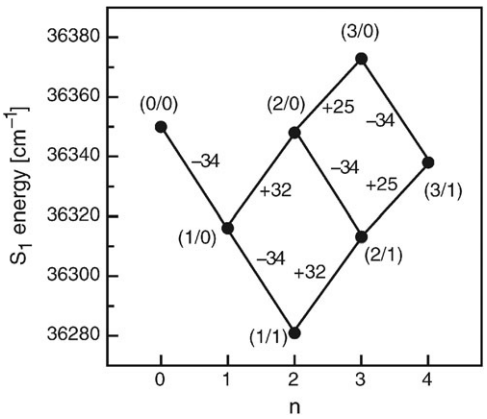

Fig. 2 Experimental S_1 origin energies derived from the 1 + 1′ REMPI spectra of PhOH–Ar$_n$ ($n \leq 4$), along with the (n/m) isomer assignments (Table 1, Fig. 1) and the incremental shifts (in cm^{-1}) employed in the additivity model.

3.2 Nanosecond IR spectra in S_0

The nanosecond IR dip spectra of PhOH–Ar$_n$ with $n \leq 4$ in the OH and CH stretch ranges (ν_{OH}, ν_{CH}) of the S_0 state are compared in Fig. 3. Although the IR spectra were obtained in the frequency range 2650–3850 cm^{-1}, only the spectral ranges revealing IR transitions are reproduced in Fig. 3. The S_1 resonances used for the ionization process are 36 350, 36 316, 36 281, 36 373, and 36 338 cm^{-1} for $n = 0$–4, respectively, which are assigned to the S_1 origins of PhOH and the (1/0), (1/1), (3/0), and (3/1) isomers of PhOH–Ar$_n$($n\pi$), respectively. The IR spectra in the OH stretch range for $n = 0$–2 are in good agreement with previous reports.[19,39] The OH stretch mode shifts slightly to a lower frequency upon attachment of π-bonding Ar ligands. The small but noticeable shifts are consistent with the weak interaction of π-bonded Ar ligands with the OH bond. The significant total redshift of $\Delta\nu_{OH} = -4$ cm^{-1} for the (3/0) isomer of PhOH–Ar$_3$(3π) may be taken as evidence for the close proximity of one of the Ar ligands and the OH group, which is expected for the assumed parallel structure of the Ar$_3$ triangle and PhOH. Comparison with the corresponding shift of the H-bonded PhOH–N$_2$(H) dimer, $\Delta\nu_{OH} = -5$ cm^{-1},[19] might also lead to the conclusion

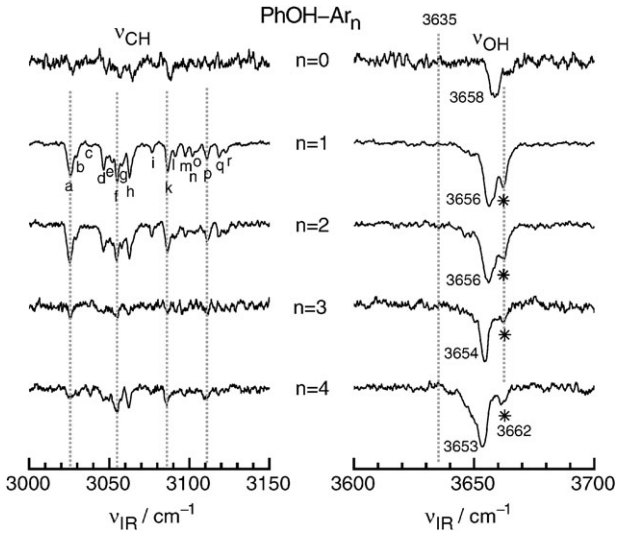

Fig. 3 Nanosecond IR dip spectra of PhOH–Ar$_n$ ($n \leq 4$) in the S_0 state in the vicinity of the OH and CH stretch fundamentals (ν_{OH}, ν_{CH}). The S_1 resonances used for the ionization process are 36 350, 36 316, 36 281, 36 373, and 36 338 cm^{-1} for n = 0–4, which are assigned to the S_1 origins of PhOH and the (1/0), (1/1), (3/0), and (3/1) isomers of PhOH–Ar$_n$($n\pi$), respectively. For the PhOH–Ar$_n$ clusters with $n \geq 1$, ν_{ION} was set to 32 260 cm^{-1} to ensure soft ionization. The asterisks indicate a Fermi resonance of a combination band with ν_{OH}. The ν_{OH} frequency observed in an Ar matrix (3635 cm^{-1}) is indicated by a dotted line. Vertical dotted lines are included to guide the eye. The transition frequencies of the bands labelled a–r in the ν_{CH} range of the n = 1 spectrum are listed in Table 2.

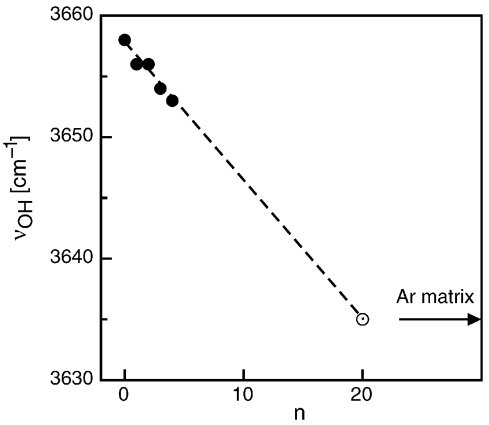

Fig. 4 Experimental ν_{OH} frequencies of PhOH–Ar$_n$ in the S_0 state as a function of the cluster size n (filled circles). The open circle and the arrow indicate that the ν_{OH} frequency observed in an Ar matrix ($n \rightarrow \infty$, ν_{OH} = 3635 cm^{-1})[42] is reached by linear extrapolation of the $n \leq 4$ data at $n \approx 20$, which corresponds roughly to the size of the first solvation shell.

Table 2 Frequencies (in cm^{-1}) of the bands observed in the IR dip spectrum of PhOH–Ar in the CH stretch range (Fig. 3)

Band	a	b	c	d	e	f	g	h	i
ν	3026	3030	3038	3046	3052	3055	3058	3063	3077
Band	k	l	m	n	o	p	q	r	
ν	3087	3091	3098	3102	3105	3111	3119	3123	

that one of the Ar ligands in the considered PhOH–Ar$_3$ isomer is H-bonded, *i.e.* PhOH–Ar$_3$(H/2π). However, the recent photoionization and photofragmentation studies of this particular PhOH–Ar$_3$ isomer clearly demonstrate that all Ar ligands are π-bonded for n = 3, PhOH–Ar$_3$(3π).[32] Moreover, the ν_{OH} band of PhOH observed in an Ar matrix ($n \rightarrow \infty$, ν_{OH} = 3635 cm^{-1}) displays a redshift of $\Delta\nu_{OH}$ = −23 cm^{-1}, *i.e.* the interaction of PhOH with mainly the first Ar solvation shell is significantly enhanced upon ν_{OH} excitation.[42] Under the very crude assumption that each Ar atom in the first solvation shell generates roughly the same $\Delta\nu_{OH}$ shift and that only the first solvation shell contributes to the matrix shift, $n \approx 20$ Ar atoms can be accommodated around PhOH in this first shell (Fig. 4). This size of the first solvation shell in PhOH–Ar$_n$ is in good agreement with that derived previously for the isoelectronic aniline–Ar$_n$ cluster series (n = 22) from mass spectrometry and electronic spectroscopy.[43] There is a further band in the OH stretch range at 3662 cm^{-1}, which is independent of the Ar cluster size (marked by an asterisk). It is assigned to a combination band, which is in Fermi resonance with the ν_{OH} fundamental. Thus, it decreases in relative intensity as the ν_{OH} frequency is reduced for increasing n.

The IR spectra of PhOH–Ar$_n$ in the CH stretch range are rich in structure and display more than 15 transitions in the frequency range 3020–3130 cm^{-1}, denoted a–r in Fig. 3. Clearly, the IR spectra in this range are heavily congested due to substantial Fermi resonances of the five possible CH stretch fundamentals (ν_{CH}) with a variety of overtone or combination bands, probably involving in-plane CH bend and CC stretch modes. There is essentially no shift of the transitions as the number of Ar atoms in PhOH–Ar$_n$ increases from n = 0 to n = 4 (<2 cm^{-1}). This observation is consistent with π-bonding Ar ligands for $n \leq 4$, which have negligible impact on the in-plane CH stretch, CH bend, and CC bend frequencies. Table 2 lists the frequencies of all bands observed in the spectrum of PhOH–Ar, which displays the best signal-to-noise ratio of all spectra recorded. The IR spectrum of PhOH deposited in an Ar matrix reveals a single unresolved band in the CH stretch range near 3050 cm^{-1},[42] which is close to the intense narrow transitions observed for the individual PhOH–Ar$_n$ clusters.

3.3 Nanosecond IR spectra in D_0

The nanosecond IR dip spectra of PhOH$^+$–Ar$_n$ with $n \leq 4$ generated by REMPI are compared in Fig. 5 in the OH stretch range (ν_{OH}) of the D_0 state. For comparison, also IR photodissociation (IRPD) spectra of PhOH$^+$–Ar$_n$ generated by electron ionization (EI) are shown as well.[11] The S_1 resonances and ν_{ION} used for the ionization process in the IR dip spectra are the same as used for the corresponding IR spectra in the S_0 state. The frequencies and widths of all transitions observed are listed in Table 3 along with the vibrational and isomer assignments. The IR dip spectra for n = 1–2 were discussed previously.[36–39] The high-frequency peak in the n = 1 spectrum at 3537 cm^{-1} has been assigned to the free ν_{OH} of PhOH$^+$–Ar(π).[36–39] The second and somewhat broader feature at 3473 cm^{-1} has been ignored in the initial report,[36] probably because its intensity was substantially reduced due to

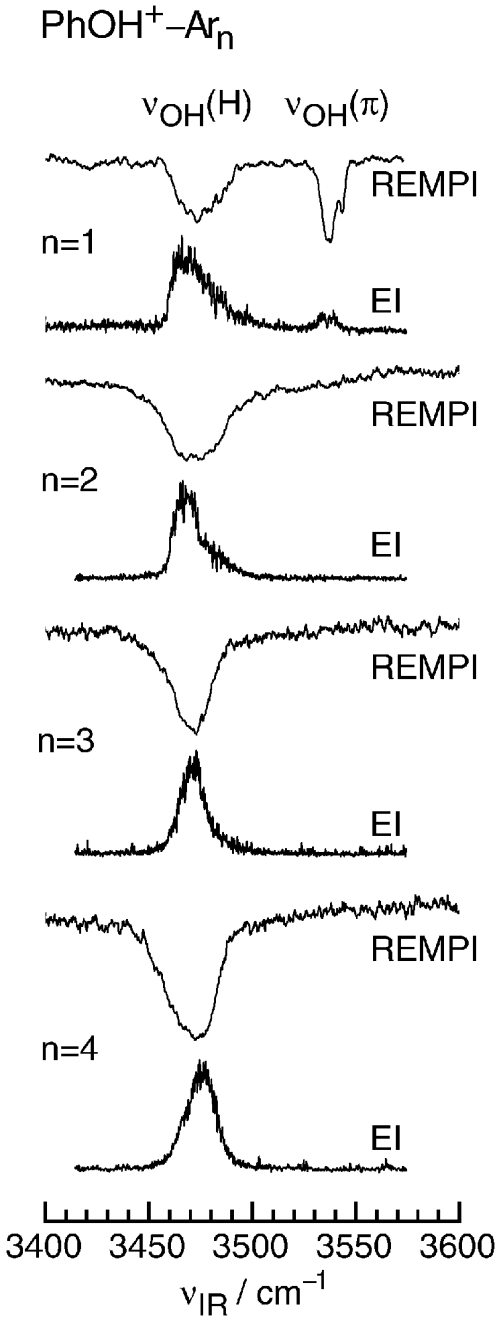

Fig. 5 Nanosecond IR dip spectra of $PhOH^+$–Ar_n (n = 1–4) in the D_0 state in the vicinity of the OH stretch fundamentals (ν_{OH}) for clusters generated by REMPI of neutral PhOH–Ar_n. The S_1 resonances used for ionization are 36 316, 36 281, 36 373, and 36 338 cm^{-1} for n = 1–4, which are assigned to the S_1 origins of the (1/0), (1/1), (3/0), and (3/1) isomers of PhOH–Ar_n($n\pi$), respectively. The ν_{ION} frequency was set to 32 260 cm^{-1} to ensure soft ionization. For comparison, also IRPD spectra of $PhOH^+$–Ar_n (n = 1–4) generated in the electron impact (EI) source are shown as well.[11] The positions and widths of the transitions are listed in Table 3, along with the vibrational and isomer assignments.

$LiNbO_3$ crystal absorptions of the IR laser system in this spectral range.[44] In a later study, this feature was tentatively attributed to a hot band transition without further specification.[39] The current interpretation is based on a recent investigation of

Table 3 Positions and widths (FWHM, in parentheses) of the ν_{OH} transitions (in cm^{-1}) observed in the IR dip (REMPI) and IRPD (EI) spectra shown in Fig. 5, along with the vibrational and isomer assignments

n	IR dip (REMPI)	IRPD (EI)[a]	Assignment
1	3537 (11)	3536 (10)	ν_{OH} of PhOH–Ar(π)
1	3473 (25)	3464 (12)	ν_{OH} of PhOH–Ar(H)
2	3474 (30)	3467 (15)	ν_{OH} of PhOH–Ar_2(H/π)
3	3472 (20)	3470 (13)	ν_{OH} of PhOH–Ar_3(H/2π)
4	3471 (28)	3475 (15)	ν_{OH} of PhOH–Ar_4(H/3π)

[a] Ref. 11.

the related $PhOH^+$–Kr dimer[40,44] and suggests an assignment to ν_{OH} excitation of a hot H-bonded $PhOH^+$–Ar(H) dimer. This isomer is generated *via* π → H isomerization triggered by ionization. As a consequence of the considerable internal energy available after isomerization, the ν_{OH} band of hot $PhOH^+$–Ar(H) results from sequence transitions and is thus somewhat blueshifted by +11 cm^{-1} from the ν_{OH} fundamental of cold $PhOH^+$–Ar(H) generated in the EI source (3464 cm^{-1}).[11] Moreover, the width of the ν_{OH} band of hot $PhOH^+$–Ar(H) generated by REMPI is much larger than that of cold $PhOH^+$–Ar(H) generated in the EI source (25 *vs.* 12 cm^{-1}). Significantly, the relative intensities of the two isomers, $PhOH^+$–Ar(π) and $PhOH^+$–Ar(H), are also rather different in both experiments. In the IR dip experiment, the relative intensities of the two ν_{OH} bands are mainly governed by the equilibrium population of the H-bound and π-bound configurations given by the rate constants of the π → H isomerization and H → π back reactions established tens of picoseconds

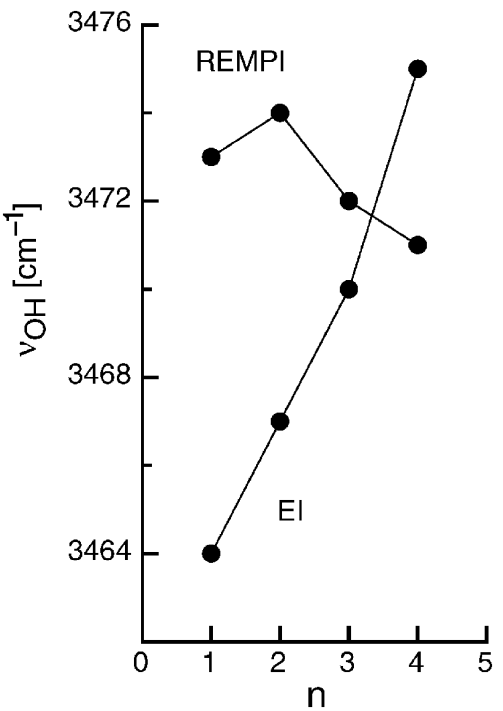

Fig. 6 Plot of the experimental ν_{OH} frequencies of $PhOH^+$–Ar_n(H/[n−1]π) as a function of the cluster size n, as measured in the IR spectra, in which the cluster ions are generated by REMPI and by EI (Fig. 5, Table 3).

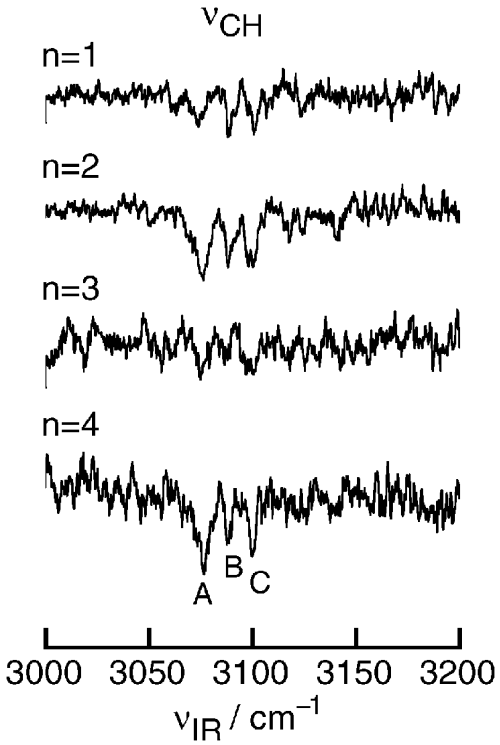

Fig. 7 Nanosecond IR dip spectra of $PhOH^+–Ar_n$ (n = 1–4) in the D_0 state in the vicinity of the CH stretch fundamentals (ν_{CH}) for clusters generated by REMPI of neutral $PhOH–Ar_n$. The S_1 resonances used for ionization are 36 316, 36 281, 36 373, and 36 338 cm^{-1} for n = 1–4, which are assigned to the S_1 origins of the (1/0), (1/1), (3/0), and (3/1) isomers of $PhOH–Ar_n(n\pi)$, respectively. The ν_{ION} frequency was set to 32 260 cm^{-1} to ensure soft ionization. The transitions A–C occur at 3077, 3088, and 3100 cm^{-1}, respectively.

after resonant ionization of neutral PhOH–Ar(π).[40] In the EI experiment, the relative intensities are mainly controlled by the relative stabilities of the two isomers and the effective temperature of the EI ion source.[11,35] The latter experiments clearly show that $PhOH^+$–Ar(H) is more stable than $PhOH^+$–Ar(π).

The IR dip spectra of $PhOH^+–Ar_n$ with n = 2–4 generated by resonant ionization of neutral $PhOH–Ar_n(n\pi)$ with only π-bonded Ar ligands display only single peaks with maxima at 3474, 3472, and 3471 cm^{-1}. These transitions are close to the ν_{OH} band of $PhOH^+$–Ar(H), indicating that one Ar ligand is H-bonded to the OH group. No signal is detected in the vicinity of the ν_{OH} band of $PhOH^+$–Ar(π) near 3535 cm^{-1}. This observation suggests that for all $PhOH–Ar_n(n\pi)$ clusters with $n \geq 2$ the π → H isomerization reaction leading to the formation of $PhOH^+–Ar_n(H/[n-1]\pi)$ occurs with 100% efficiency and without any back reaction.[39] This π → H switch releases internal energy into the cluster, so that the widths of the ν_{OH} bands of these clusters are larger (typically by a factor of 2) than those observed for the corresponding cold $PhOH^+–Ar_n(H/[n-1]\pi)$ species generated by EI (Table 3). Interestingly, the ν_{OH} bands of $PhOH^+–Ar_n(H/[n-1]\pi)$ generated by REMPI shift slightly to lower frequencies with increasing n, whereas the opposite trend is observed for the cold clusters produced by EI.[8,11] In addition, the maxima of the ν_{OH} bands observed using the two different techniques

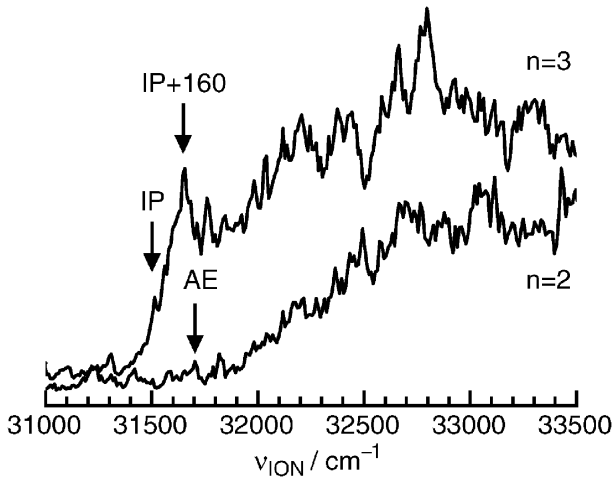

Fig. 8 PIE spectra of $PhOH–Ar_3$ recorded *via* resonant excitation of the S_1 origin at 36 373 cm^{-1} (assigned to the (3/0) isomer) and monitored in the $PhOH^+–Ar_3$ parent and $PhOH^+–Ar_2$ fragment channels. The arrows indicate the positions of the ionization potential (IP) and the appearance energy of fragmentation (AE) at $\nu_{ION} \approx$ 31 500 and 31 700 cm^{-1}, respectively. For the picosecond experiment illustrated in Fig. 9, ν_{ION} was set to 31 660 cm^{-1}, which corresponds to IP + 160 cm^{-1}.

approach each other for increasing cluster size, demonstrating that the difference in the internal energy content between both cluster species decreases relative to the total internal energy (Fig. 6).

The IR dip spectra of $PhOH^+–Ar_n$ with $n \leq 4$ generated by REMPI are compared in Fig. 7 in the CH stretch range (ν_{CH}) of the D_0 state (3000–3200 cm^{-1}). Three transitions denoted A–C are identified in this frequency range at 3077, 3088, and 3100 cm^{-1}, respectively. As for neutral $PhOH–Ar_n$, the positions do not vary with n within the experimental resolution. Thus, the observed frequencies closely approximate those of isolated $PhOH^+$ (messenger technique).[45–48] In general, ionization of PhOH leads to an increase in the CH stretch frequencies and a substantial decrease in its oscillator strength. Due to the latter effect, the ν_{CH} fundamentals of $PhOH^+$ have escaped previous detection.[10] In contrast to neutral PhOH, the ν_{CH} spectral range is not complicated by Fermi resonances for the cation species. The ν_{CH} frequencies of $PhOH^+$ are close to those of the benzene cation (ν_{CH} = 3094 cm^{-1}),[46,49] suggesting that there is little impact of the OH group on the CH bond strength. Unfortunately, there appears to be no IR spectroscopic study available for $PhOH^+$ embedded in an Ar matrix, preventing at this stage any comparison of the $PhOH^+–Ar_n$ cluster data in the ν_{CH} and ν_{OH} stretch ranges with the bulk limit.

3.4 PIE spectra of $PhOH–Ar_3$

PIE spectra recorded *via* the S_1 origin of the (3/0) isomer of $PhOH–Ar_3(3\pi)$ at 36 373 cm^{-1} and monitored in the $PhOH^+–Ar_3$ parent and the $PhOH^+–Ar_2$ daughter channel are reproduced in Fig. 8. The field-corrected adiabatic ionization potential for n = 3 (IP = 68 060 ± 50 cm^{-1}) and the appearance energy for fragmentation into n = 2 (AE = 68 260 ± 50 cm^{-1}) agree well with a recent report.[32] As discussed previously,[32,37,39] the rather low appearance threshold of 200 cm^{-1} for fragmentation

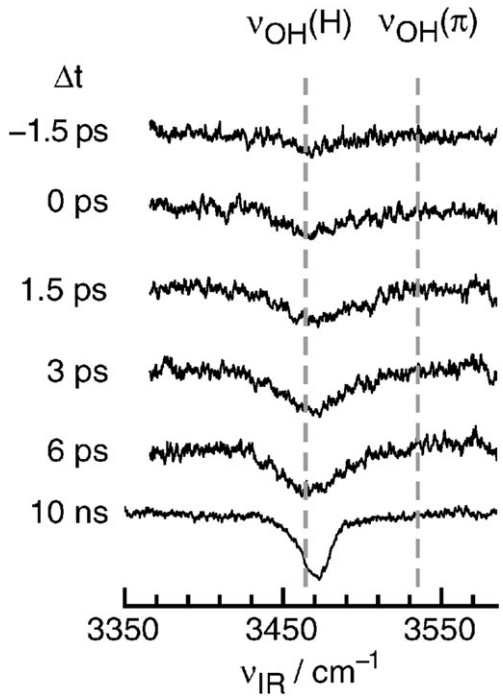

Fig. 9 Picosecond time-resolved IR dip spectra of $PhOH^+$–Ar_3 as a function of the delay time Δt after the ionization process. The $PhOH^+$–Ar_3 clusters are generated by resonant excitation of the S_1 origin of the (3/0) isomer of PhOH–$Ar_3(3\pi)$ at 36 373 cm^{-1}. The frequency of ν_{ION} was set to 31 660 cm^{-1}, which corresponds to IP + 160 cm^{-1} (Fig. 8). For comparison, the IR spectrum obtained with the nanosecond laser system is also shown (*i.e.* Δt = 10 ns). The positions of the $\nu_{OH}(H)$ and $\nu_{OH}(\pi)$ resonances of $PhOH^+$–Ar at 3464 and 3536 cm^{-1} as obtained in the EI experiment are indicated by dashed lines (Fig. 5, Table 1).[11]

is a clear signature for the ionization-induced $\pi \rightarrow H$ isomerization process, in which one of the π-bonded Ar ligands of $PhOH^+$–$Ar_3(3\pi)$ isomerizes to the OH site yielding $PhOH^+$–$Ar_3(H/2\pi)$. The binding energy of a π-bonded Ar ligand to $PhOH^+$ is ~535 cm^{-1},[25] whereas the strength of the H-bond of Ar to $PhOH^+$ is ~870 cm^{-1}.[32] Thus, the difference of the binding energies at the H-bound and π-bound sites (~335 cm^{-1}) is released into other degrees of freedom in the cluster and becomes available for dissociation of another π-bonded Ar ligand. Consequently, $\pi \rightarrow H$ isomerization reduces the dissociation threshold of a π-bound ligand from ~535 cm^{-1} to ~200 cm^{-1}, in agreement with the experimental observation in Fig. 8.[32] Significantly, this energetic result confirms that the initially prepared and ionized n = 3 cluster has no H-bonded ligand, *i.e.* it is of the form PhOH–$Ar_3(3\pi)$.

3.5 Picosecond IR spectra of $PhOH^+$–Ar_3 in D_0

In order to investigate the rate of the $\pi \rightarrow H$ isomerization reaction triggered by ionization of the (3/0) isomer of PhOH–$Ar_3(3\pi)$, IR dip spectra have been measured in the ν_{OH} range of the cation ground state using picosecond lasers. To this end, the ps UV lasers are fixed at ν_{UV} = 36 373 cm^{-1} and ν_{ION} = 31 660 cm^{-1} in order to ensure resonant soft ionization of this particular isomer with an ionization excess energy of 160 cm^{-1} (Fig. 8). The ps IR laser is then scanned through the ν_{OH} range at various delay times Δt with respect to the ionization event. The resulting IR spectra obtained for Δt ranging from −1.5 to +6 ps are compared in Fig. 9. The corresponding spectrum obtained with nanosecond lasers at Δt = 10 ns is similar in appearance as the one obtained at 6 ps. It displays a better spectral resolution owing to the longer laser pulses employed. For comparison, the ν_{OH} resonances for $PhOH^+$–Ar(H) and $PhOH^+$–Ar(π) generated in the electron impact source at $\nu_{OH}(H)$ = 3464 cm^{-1} and $\nu_{OH}(\pi)$ = 3536 cm^{-1} are also indicated.[33] As is evident from Fig. 9, the $\nu_{OH}(H)$ resonance grows rapidly at very short delay times and is already fully developed at $\Delta t \approx$ 3ps. As the time resolution of the ps laser system is of similar magnitude (3 ps), the time-resolved IR spectra in Fig. 9 provide only an upper limit for the $\pi \rightarrow H$ isomerization time constant, $\tau \leq$ 3 ps. No distinct signal can be identified in the $\nu_{OH}(\pi)$ range even for very short delay times. This observation supports the conclusion of the fast $\pi \rightarrow H$ switch. In addition, the IR oscillator strength of $\nu_{OH}(H)$ is a factor of ~2–3 higher than that of $\nu_{OH}(\pi)$.[33,44] Moreover, the spectral width of the $\nu_{OH}(H)$ band is significantly larger than that of $\nu_{OH}(\pi)$.[11] Both aspects clearly enhance the detection efficiency of the $\nu_{OH}(H)$ band in comparison to $\nu_{OH}(\pi)$ in the picosecond experiments and may partly explain the lack of distinct detection of $\nu_{OH}(\pi)$ at early delay, $\Delta t \approx 0$. However, although the signal-to-noise ratio for long delay times (*e.g.*, for Δt = 6 ps) is appreciable, no signal is detected in the $\nu_{OH}(\pi)$ range. This observation indicates that the yield for the $\pi \rightarrow H$ isomerization is (near) unity, *i.e.*, there is no sign for the $H \rightarrow \pi$ back reaction. This result is similar to the case of $PhOH^+$–Ar_2,[38,39] and is rationalized by efficient intracluster vibrational energy redistribution (IVR) occurring after the $\pi \rightarrow H$ switch. Interestingly, for the $PhOH^+$–Kr dimer, the $H \rightarrow \pi$ back reaction can be observed leading to the detection of the $\nu_{OH}(\pi)$ band even for delay times as long as 20 ns.[40,44] The same conclusion holds for $PhOH^+$–Ar (Fig. 5). Apparently, for $PhOH^+$–Kr/Ar the density of states is too small for efficient IVR to occur after the initial $\pi \rightarrow H$ switch triggered by ionization, leading to an equilibrium population of H-bound and π-bound configurations given by the rate constants of the $\pi \rightarrow H$ and $H \rightarrow \pi$ reactions. In contrast, fast IVR prevents the $H \rightarrow \pi$ back reaction for $PhOH^+$–Ar_n with n = 2 and 3 due to the large increase in the density of states (mainly arising from the additional low-frequency van der Waals modes), eventually leading to a complete decay of the π population according to an exponential time evolution.[38,39,50]

Finally, it is interesting to compare the $\pi \rightarrow H$ switching rates derived for the individual systems. The rate constant for the $\pi \rightarrow H$ switch in $PhOH^+$–Kr (k = 0.05 ps^{-1}, $\tau = 1/k$ = 20 ps)[40] is three times lower than for $PhOH^+$–Ar_2 (k = 0.14 ps^{-1}, τ = 7 ps),[39] mainly due to the heavier mass of Kr. On the other hand, the rate for $PhOH^+$–Ar_3 ($k > 0.3$ ps^{-1}, $\tau \leq$ 3 ps) is faster than for $PhOH^+$–Ar_2, because the isomerization pathway for the $\pi \rightarrow H$ motion is shorter in the former cluster. Depending on the exact structure of the (3/0) isomer of $PhOH^+$–$Ar_3(3\pi)$, the distance from the nearest π-bound Ar ligand to the OH site is by a factor of 1.5–2 shorter than for the (1/1) isomer of $PhOH^+$–$Ar_2(2\pi)$.

4. Conclusions

REMPI spectra of the $S_1 \leftarrow S_0$ transition of PhOH–Ar_n with $n \leq 4$ are analysed using a simple additivity model to rationalize the S_1 origin shifts upon sequential complexation at various π binding sites. The application of this model has allowed for the identification of two local minimum structures not recognized previously, namely the (2/0) isomer for $n = 2$ and the (2/1) isomer for $n = 3$. The model has also been used to assign the observed S_1 origin of the $n = 4$ spectrum to the (3/1) isomer. Future experiments to support the new isomer assignments include high-resolution excitation spectroscopy at the level of rotational resolution,[21] and the measurement of photoionization thresholds, which are expected to also follow certain additivity rules.[2] Furthermore, *ab initio* calculations for PhOH–Ar_n are underway for $n \leq 4$, in order to predict the ΔS_1 shifts and the intermolecular vibrational structure observed in the S_1 state. IR spectra of neutral PhOH–Ar_n recorded in the range of the OH and CH stretch fundamentals (ν_{OH}, ν_{CH}) of the S_0 state are consistent with cluster structures, in which all Ar ligands are π-bonded, PhOH–$Ar_n(\pi)$. The small but noticeable incremental $\Delta\nu_{OH}$ shifts are compatible with a first solvation shell size of $n \approx 20$. The ν_{CH} stretch region is heavily congested due to a plethora of Fermi resonances. In contrast to neutral PhOH–Ar_n, the IR spectra of the $PhOH^+$–Ar_n cations generated by resonant photoionization of the neutral precursor display the signature of H-bonded isomers, suggesting that ionization triggers a $\pi \rightarrow H$ isomerization reaction, in which one of the π-bonded Ar ligands moves toward the more attractive OH site. The dynamics of this isomerization reaction is measured for the (3/0) isomer of PhOH–$Ar_3(3\pi)$ by picosecond time-resolved IR spectroscopy, yielding a time constant of $\tau \leq 3$ ps ($k > 0.3$ ps^{-1}) for the $\pi \rightarrow H$ switching reaction toward the $PhOH^+$–$Ar_3(H/2\pi)$ isomer. Due to the high density of intermolecular states of this tetrameric cluster, IVR prevents any $H \rightarrow \pi$ back reaction.

Acknowledgements

This work was supported by a Grant-in-Aid for Scientific Research KAKENHI in the priority area 477 from MEXT (Japan), the Core-to-Core Program of the Japan Society for Promotion of Science, and the *Deutsche Forschungsgemeinschaft* (DO 729/4). M.S. is grateful for a NaFöG Fellowship.

References

1 P. Hobza and K. Müller-Dethlefs, *Non-Covalent Interactions*, The Royal Society of Chemistry, Cambridge, 2010.
2 N. Gonohe, H. Abe, N. Mikami and M. Ito, *J. Phys. Chem.*, 1985, **89**, 3642.
3 K. Müller-Dethlefs, O. Dopfer and T. G. Wright, *Chem. Rev.*, 1994, **94**, 1845.
4 T. Ebata, A. Fujii and N. Mikami, *Int. Rev. Phys. Chem.*, 1998, **17**, 331.
5 K. Kleinermanns, M. Gerhards and M. Schmitt, *Ber. Bunsen-Ges. Phys. Chem.*, 1997, **101**, 1785.
6 C. E. H. Dessent and K. Müller-Dethlefs, *Chem. Rev.*, 2000, **100**, 3999.
7 K. Müller-Dethlefs and P. Hobza, *Chem. Rev.*, 2000, **100**, 143.
8 O. Dopfer, *Z. Phys. Chem.*, 2005, **219**, 125.
9 O. Dopfer, M. Melf and K. Müller-Dethlefs, *Chem. Phys.*, 1996, **207**, 437.
10 A. Fujii, T. Ebata and N. Mikami, *J. Phys. Chem. A*, 2002, **106**, 8554.
11 N. Solcà and O. Dopfer, *J. Phys. Chem. A*, 2001, **105**, 5637.
12 N. Solcà and O. Dopfer, *Eur. Phys. J. D*, 2002, **20**, 469.
13 F. Pasker, N. Solcà and O. Dopfer, *J. Phys. Chem. A*, 2006, **110**, 12793.
14 Q. L. Gu and J. L. Knee, *J. Chem. Phys.*, 2008, **128**, 064311.
15 A. Patzer, J. Langer, H. Knorke, H. Neitsch, O. Dopfer, M. Miyazaki, K. Hattori, A. Takeda, S. I. Ishiuchi and M. Fujii, *Chem. Phys. Lett.*, 2009, **474**, 7.
16 H. S. Andrei, N. Solca and O. Dopfer, *Phys. Chem. Chem. Phys.*, 2004, **6**, 3801.
17 H. S. Andrei, N. Solca and O. Dopfer, *J. Phys. Chem. A*, 2005, **109**, 3598.
18 N. Solcà and O. Dopfer, *J. Am. Chem. Soc.*, 2004, **126**, 1716.
19 A. Fujii, M. Miyazaki, T. Ebata and N. Mikami, *J. Chem. Phys.*, 1999, **110**, 11125.
20 S. I. Ishiuchi, Y. Tsuchida, O. Dopfer, K. Müller-Dethlefs and M. Fujii, *J. Phys. Chem. A*, 2007, **111**, 7569.
21 I. Kalkman, C. Brand, C. Vu, W. L. Meerts, Y. N. Svartsov, O. Dopfer, K. Müller-Dethlefs, S. Grimme and M. Schmitt, *J. Chem. Phys.*, 2009, **130**, 224303.
22 J. Makarewicz, *J. Chem. Phys.*, 2006, **124**, 084310.
23 J. Cerny, X. Tong, P. Hobza and K. Müller-Dethlefs, *Phys. Chem. Chem. Phys.*, 2008, **10**, 2780.
24 M. A. Vincent, I. H. Hillier, C. A. Morgado, N. A. Burton and X. Shan, *J. Chem. Phys.*, 2008, **128**, 044313.
25 C. E. H. Dessent, S. R. Haines and K. Müller-Dethlefs, *Chem. Phys. Lett.*, 1999, **315**, 103.
26 S. R. Haines, C. E. H. Dessent and K. Müller-Dethlefs, *J. Electron Spectrosc. Relat. Phenom.*, 2000, **108**, 1.
27 A. Armentano, X. Tong, M. Riese, S. E. Pimblott, K. Müller-Dethlefs, M. Fujii and O. Dopfer, *Phys. Chem. Chem. Phys.*, 2011, DOI: 10.1039/c004497k.
28 M. Schmidt, M. Mons and J. Le Calve, *Z. Phys. D, At., Mol. Clusters*, 1990, **17**, 153.
29 M. Schmidt, M. Mons and J. Lecalve, *Chem. Phys. Lett.*, 1991, **177**, 371.
30 P. Hermine, P. Parneix, B. Coutant, F. G. Amar and P. Bréchignac, *Z. Phys. D, At., Mol. Clusters*, 1992, **22**, 529.
31 S. Douin, S. Piccirillo and P. Bréchignac, *Chem. Phys. Lett.*, 1997, **273**, 389.
32 A. Armentano, M. Riese, M. Taherkhani, M. B. Yezzar, K. Müller-Dethlefs, M. Fujii and O. Dopfer, *J. Phys. Chem. A*, 2010, **114**, 11139.
33 N. Solcà and O. Dopfer, *Chem. Phys. Lett.*, 2000, **325**, 354.
34 N. Solcà and O. Dopfer, *Chem. Phys. Lett.*, 2003, **369**, 68.
35 N. Solcà and O. Dopfer, *J. Mol. Struct.*, 2001, **563/564**, 241.
36 A. Fujii, T. Sawamura, S. Tanabe, T. Ebata and N. Mikami, *Chem. Phys. Lett.*, 1994, **225**, 104.
37 X. Tong, A. Armentano, M. Riese, M. B. Yezzar, S. E. Pimblott, K. Müller-Dethlefs, S. Ishiuchi, M. Sakai, A. Takeda, M. Fujii and O. Dopfer, *J. Chem. Phys.*, 2010, **133**, 154308.
38 S. Ishiuchi, M. Sakai, Y. Tsuchida, A. Takeda, Y. Kawashima, M. Fujii, O. Dopfer and K. Müller-Dethlefs, *Angew. Chem., Int. Ed.*, 2005, **44**, 6149.
39 S. I. Ishiuchi, M. Sakai, Y. Tsuchida, A. Takeda, Y. Kawashima, O. Dopfer, K. Muller-Dethlefs and M. Fujii, *J. Chem. Phys.*, 2007, **127**, 114307.
40 M. Miyazaki, A. Takeda, S. Ishiuchi, M. Sakai, O. Dopfer and M. Fujii, *Phys. Chem. Chem. Phys.*, 2010, DOI: 10.1039/c0cp01961e.
41 C. Crepin and A. Tramer, *Chem. Phys.*, 1991, **156**, 281.
42 A. M. Plokhotnichenko, E. D. Radchenko, Y. P. Blagoi and V. A. Karachevtsev, *Low Temp. Phys.*, 2001, **27**, 666.
43 T. Pino, P. Parneix, S. Douin and P. Brechignac, *J. Phys. Chem. A*, 2004, **108**, 7364.
44 A. Takeda, H. S. Andrei, M. Miyazaki, S. I. Ishiuchi, M. Sakai, M. Fujii and O. Dopfer, *Chem. Phys. Lett.*, 2007, **443**, 227.
45 M. Okumura, L. I. Yeh, J. D. Myers and Y. T. Lee, *J. Phys. Chem.*, 1990, **94**, 3416.
46 O. Dopfer, R. V. Olkhov and J. P. Maier, *J. Chem. Phys.*, 1999, **111**, 10754.
47 A. Fujii, E. Fujimaki, T. Ebata and N. Mikami, *J. Chem. Phys.*, 2000, **112**, 6275.
48 E. J. Bieske and O. Dopfer, *Chem. Rev.*, 2000, **100**, 3963.
49 N. Solcà and O. Dopfer, *J. Phys. Chem. A*, 2003, **107**, 4046.
50 C. Walter, R. Kritzer, A. Schubert, C. Meier, O. Dopfer and V. Engel, *J. Phys. Chem. A*, 2010, **114**, 9743.

